

Title No. 113-S07

Behavior of Steel Fiber-Reinforced Concrete under Reversed Cyclic Shear

by Jun Wei Luo and Frank J. Vecchio

It is well known that the monotonic behavior of reinforced concrete can be improved with the addition of steel fibers. However, available literature on the use of steel fibers as shear or flexural reinforcement has predominantly focused on non-seismic applications.

Experiments were performed to characterize the reversed cyclic response of steel fiber-reinforced concrete (SFRC) and compare its response with that of monotonically loaded SFRC and conventionally reinforced concrete. Ten concrete panels were constructed and tested under in-plane pure-shear loading conditions. The test parameters included fiber volume content, fiber aspect ratio, and loading protocol. Results indicate that, under reversed cyclic loading, SFRC exhibits stable hysteretic response with minimal strength degradation and no noticeable changes in ductility. Fiber volume content and fiber aspect ratio are found to significantly influence the shear performance of SFRC. Details and results are provided.

Keywords: fiber-reinforced concrete; hysteretic response; reversed cyclic; shear; steel fibers.

INTRODUCTION

The idea of including steel fibers in concrete can be dated back to the 1800s when metallic waste was added to concrete.¹ The randomly distributed and discontinuous characteristics of fibers allow cracks in any direction to be bridged and permit improved stress transfer across cracks. This fiber bridging allows crack openings to be controlled, enabling the development of additional cracks. In turn, this reduces the crack width and crack spacing, increasing post-cracked ductility and energy absorption capacity.²⁻⁴ Despite the aforementioned benefits, steel fiber-reinforced concrete (SFRC) has seen limited structural usage and has had some acceptance as primary reinforcement in flexural-critical structural members only; use in shear-critical members, especially under seismic applications, is uncommon.^{5,6}

In past decades, a significant amount of research into the shear behavior of SFRC beams under monotonic loading was conducted.^{7,8} The results of these studies led to the permitted exemption of SFRC beams from minimum shear reinforcement requirement in the ACI Building Code.⁹ This exemption is supported by the database of 147 monotonically loaded SFRC beams compiled by Parra-Montesinos.⁷ The database shows SFRC without stirrups and with at least 0.75% fiber volume fraction exhibited a normalized shear stress at failure larger than $0.3\sqrt{f'_c}$ MPa ($3.6\sqrt{f'_c}$ psi)—a value significantly higher than the expected shear contribution from plain concrete. In some cases, an addition of 0.5% to 1.0% short steel fibers (fiber length = 30 mm [1.2 in.]) was sufficient in altering the beam's failure mode from shear to flexure.^{10,11}

Susetyo et al.⁸ investigated the monotonic shear behavior of SFRC elements through a series of 10 panel tests. The test results show that fibers significantly improve the post-

cracking tensile behavior and cracking characteristics of concrete. The results also illustrate the importance of fiber type and fiber volume content. Concrete with high-aspect-ratio fibers or high fiber volume fractions resulted in much improved shear resistance, post-cracking deformation capacity, and crack control characteristics.

Cyclic loading is one of the most challenging cases of loading, both in structural performance and from a modeling perspective. Although limited research has been done to investigate the behavior of SFRC under reversed cyclic loading, many of these studies conclude positive effects are attained from the addition of steel fibers in reinforced concrete.¹²⁻¹⁴

Research conducted on shear-critical cyclic beam tests performed by Chalioris¹² shows that the addition of long end-hooked steel fibers increases the ultimate load, ultimate drift, and energy dissipation of the beams. The addition of 0.75% by volume of fibers can alter the failure mode of the cyclically loaded beam from a shear failure to a more ductile shear-flexure failure. Further, the addition of a low fiber volume (0.5%) to plain concrete improved the cyclic strength degradation from 20% (plain concrete) to 14% (SFRC).

Tests on six large-scale slender coupling beams performed by Setkit¹³ showed that SFRC beams subjected to large shear reversals can exhibit a stable hysteretic behavior despite the reduced diagonal and confinement reinforcement. The addition of a high fiber volume fraction (1.5%) led to a 13% increase in strength and a 64% increase in the total maximum drift.

Carnovale and Vecchio¹⁴ performed a pilot investigation on the cyclic behavior of SFRC elements, and one SFRC panel under reversed cyclic in-plane shear was included in the test matrix. Compared to the monotonically loaded companion panel, the cyclically loaded SFRC panel experienced 25% strength degradation and 52% reduction in the peak shear strain. This severe detrimental effect of the cycling of load is contrary to the behavior of cyclically loaded shear-critical beams, as noted previously. Further research is necessary to understand, and provide confidence in, the cyclic shear response of SFRC.

RESEARCH SIGNIFICANCE

Cyclically loaded reinforced concrete members are typically heavily reinforced with difficult detailing requirements. There is growing demand to reduce these requirements

ACI Structural Journal, V. 113, No. 1, January-February 2016.

MS No. S-2014-317.R1, doi: 10.14359/51687940, received February 7, 2015, and reviewed under Institute publication policies. Copyright © 2016, American Concrete Institute. All rights reserved, including the making of copies unless permission is obtained from the copyright proprietors. Pertinent discussion including author's closure, if any, will be published ten months from this journal's date if the discussion is received within four months of the paper's print publication.

with innovative materials. As previously noted, the addition of steel fibers has proven to be an attractive option as shear reinforcement in these critical members. However, its usage in seismic applications has been hindered by the lack of experimental data and design guidance. The panel tests performed in this work permit a more comprehensive understanding of the cyclic response of SFRC and provide data, without the obscuring effects of flexure, for developing rational constitutive models for SFRC.

EXPERIMENTAL PROGRAM

Contributing to a comprehensive study of SFRC elements subjected to reverse cyclic loading, 10 panel specimens were constructed. As outlined in Table 1, eight of the 10 panels contained SFRC, while the other two consisted of plain concrete and were the control panels. Because two identical panels were made for each concrete mixture, the test matrix can be partitioned into five pairs; each pair included a monotonically loaded and a reversed cyclically loaded panel. Three different fiber volume contents (0.5, 1.0, and 1.5%) were examined. Two types of end-hooked steel fibers (RC80/30BP and ZP305) were used to investigate the influence of fiber aspect ratio.

Table 1—Test matrix

ID	Fiber type	V_f , %	AR_f	Loading protocol
CMS	—	—	—	Monotonic
CRC	—	—	—	Reversed cyclic
F1V1MS	RC80/30BP	0.5	79	Monotonic
F1V1RC	RC80/30BP	0.5	79	Reversed cyclic
F1V2MS	RC80/30BP	1.0	79	Monotonic
F1V2RC	RC80/30BP	1.0	79	Reversed cyclic
F1V3MS	RC80/30BP	1.5	79	Monotonic
F1V3RC	RC80/30BP	1.5	79	Reversed cyclic
F2V2MS	ZP305	1.0	55	Monotonic
F2V2RC	ZP305	1.0	55	Reversed cyclic

Table 2—Concrete mixture design

Material	Plain concrete	SFRC
Type 10 cement, kg (lb)	360 (794)	480 (1058)
Water, kg (lb)	144 (317)	206 (454)
Sand, kg (lb)	847 (1867)	1114 (2456)
10 mm (0.4 in.) limestone, kg (lb)	1080 (2381)	792 (1746)
High range water reducer, mL (oz.)	2800 (94.7)	3750 (126.8)
Steel fibers, kg (lb)	—	39.3/78.5/117.8* (86.4/173.1/259.7)

*Note: Corresponds to 0.5%, 1.0%, and 1.5% fiber content, respectively.

Table 3—Properties of reinforcement

Wire type	d_b , mm (in.)	A_{s_s} , mm ² (in. ²)	E_s , GPa (ksi)	f_y , MPa (ksi)	$\epsilon_y \times 10^{-3}$	f_u , MPa (ksi)	$\epsilon_u \times 10^{-3}$
D4	5.70 (7/32)	25.5 (0.040)	190.5 (27,630)	490.6 (71.2)	2.60	639.2 (92.7)	21.8
D8	8.10 (3/8)	51.5 (0.080)	184.7 (26,788)	457.8 (66.4)	2.48	591.9 (85.8)	33.7

Materials

The dry composition per cubic meter of concrete for the two types of concrete used is shown in Table 2. Both mixtures had a target 28-day compressive strength of 50 MPa (7.3 ksi). The concrete used in this work was mixed using the facilities at the University of Toronto. The two identical panels of each pair were cast using the same batch of concrete. After casting, all panel specimens were moist-cured and covered with wet burlaps and polytarp plastic for 7 days. Afterward, the specimens were stored in open air and cured in ambient conditions until the test date. It is important to note that for the F1V3 series, with 1.5% RC80/30BP fibers, a noticeable variation in fiber concentration was observed during casting. The effect of this to the overall structural response of the panels will be discussed in the later sections.

The workability of concrete was assessed using the conventional slump cone test. The slump for the control series, F1V1 series, F1V2 series, F1V3 series, and F2V2 series was 190, 130, 90, 170, and 160 mm (7.5, 5.1, 3.5, 6.7, and 6.3 in.), respectively. The measured slumps were reasonably close to the target slump of 150 mm (5.9 in.), and all concrete exhibited good workability.

Two types of deformed reinforcing steel were used for the panel specimens. The deformed bars were cold-formed and exhibited no defined yield plateau; hence, the yield strength and strain were defined using the proportionality limit. The mechanical properties of the reinforcing steel were determined using coupon tests and are reported in Table 3.

All fibers used had a fiber length of 30 mm (1.2 in.) and, hence, the change in fiber aspect ratio was due to the difference in fiber diameter. Table 4 gives the mechanical properties of the steel fibers. It is important to note that the lower aspect ratio fiber with a larger diameter led to a reduction of fiber count by approximately half compared to a unit volume of concrete with the higher aspect ratio fiber.

Specimens

Two different reinforcement configurations were used for the 890 x 890 x 70 mm (35 x 35 x 2.75 in.) panel specimens. The control panels' reinforcement consisted of 40 D8 bars in the primary direction ($\rho_x = 3.31\%$) and 10 D4 bars in the transverse direction ($\rho_y = 0.42\%$). This transverse reinforcement ratio, though larger than the prescribed minimum shear reinforcement of many design standards, represents a relatively low amount of transverse reinforcement. To compare the behavior of SFRC and conventionally reinforced concrete, the SFRC panels had the same reinforcement layout in the primary direction, but contained no continuous bars in the transverse direction ($\rho_x = 3.31\%$, $\rho_y = 0$). Threaded rods were used in the transverse direction for all specimens to provide sufficient stress transfer to the shear keys. Figures showing the reinforcement layout can be found in the Appendix.

Table 4—Properties of fiber¹⁷

Fiber type	l_f , mm (in.)	d_f , mm (in.)	AR_f	f_{uf} , MPa (ksi)
RC80/30BP	30 (1-3/16)	0.38 (0.015)	79	2300 (333.6)
ZP305	30 (1-3/16)	0.55 (0.022)	55	1300 (188.6)

Test setup

All panels were tested under in-plane pure shear conditions using the Panel Element Tester Facility at the University of Toronto. As depicted in Fig. 1, the typical panel had 20 shear keys located around its perimeter through which load was applied. Three rigid links were connected to two of the bottom shear keys to form a pin connection and a vertical roller (refer to the Appendix). All other shear keys were connected to two hydraulic jacks; one jack applied a vertical load while the other applied a horizontal load. The vertical jacks were calibrated to produce loads of equal magnitude but in the opposite direction to those of the horizontal jacks, creating a pure shear loading condition. To prevent the panel from moving in the out-of-plane direction, a lateral support frame was provided on the back of the tester machine.

The load was applied in a quasi-static fashion under a force-control mode. For the monotonic tests, the loading was applied in the positive shear direction until failure. For the reversed cyclic tests, each cycle was composed of loading in both directions, and two load cycles were taken at each target stress level to evaluate the stiffness degradation throughout the loading history (refer to Fig. 2). Additional load stages were employed when noticeable cracking occurred. At each load stage, as the load was held constant, crack patterns were marked and crack widths were measured.

Instrumentation

The testing facility and specimens were extensively instrumented and monitored. Six linear variable displacement transducers (LVDTs) were mounted on each face of the specimen to monitor the overall deformations (refer to Fig. 1). These LVDTs allowed all strain parameters to be obtained using Mohr's Circle transformation. Four pressure transducers were used to record the pressure at various points within the hydraulic system. Each of the three rigid links was connected to a load cell to ensure the reaction forces measured were consistent with the pressure applied.

EXPERIMENTAL RESULTS AND DISCUSSION

This section presents and discusses the structural response of the 10 panel specimens. Selected results, calculated using the Disturbed Stress Field Model,¹⁵ are presented herein to illustrate the influence of steel fibers; a more comprehensive set of test observations and results are presented elsewhere.¹⁶ The analyses were primarily based on the shear response, concrete principal stress response, and crack control characteristics. All panels experienced a shear failure due to opening of shear cracks followed by a breakdown of the aggregate interlock mechanism. Failure of the SFRC panels was initiated by fiber pullout, whereas the control panels' failure was caused by yielding of the transverse reinforcement. The failure crack patterns can be found in the Appendix.

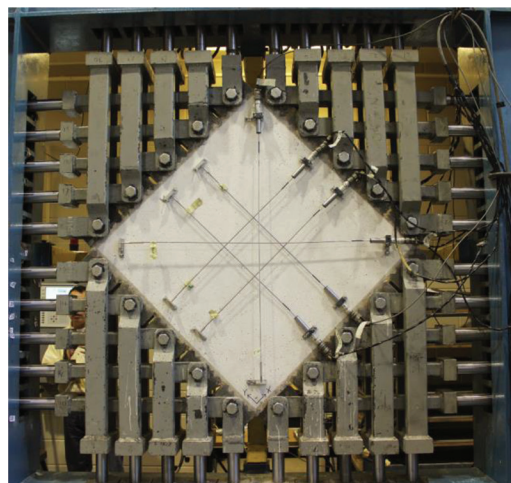


Fig. 1—Panel specimen in Panel Element Tester.

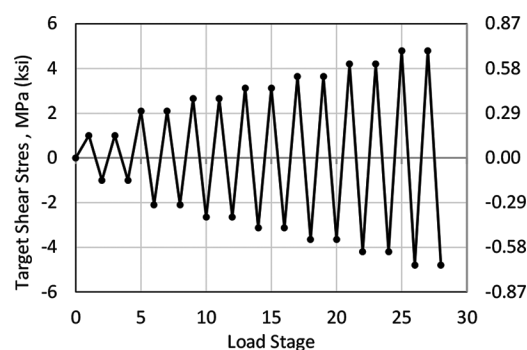


Fig. 2—Sample reversed cyclic loading protocol.

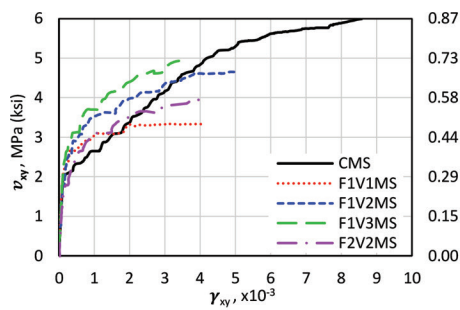
Influence of fiber type and fiber content

Shear resistance and ductility—All SFRC panels performed reasonably well in terms of the maximum shear stress, managing to withstand at least half of the maximum shear stress taken by the well-reinforced control panels (refer to Table 5). As indicated by the monotonic (that is, backbone) curves and the cyclic envelope curves in Fig. 3, concretes with higher fiber volume fractions withstood higher shear stresses. SFRC panels containing a fiber content of 1.5% managed to resist at least 82% of the maximum shear stress sustained by the conventionally reinforced panels; this was significant considering the control panels contained a shear reinforcement ratio larger than many design code's prescribed minimum. However, panels with a fiber content of 0.5% were able to sustain only 56% of the maximum shear stress of the control panels, providing inadequate shear resistance.

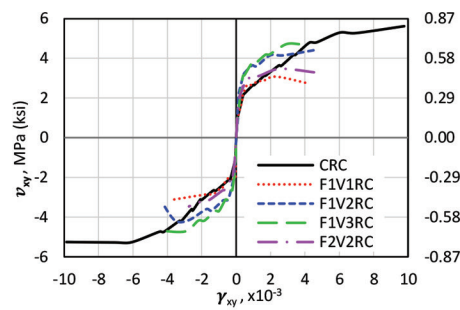
The two panels from the F2V2 series, with 1.0% ZP305 fibers, contained low-aspect-ratio fibers, which resulted in approximately the same number of fibers as concrete with 0.5% RC80/30BP fibers—the F1V1 series. Because the performance of SFRC members is strongly linked to the number of fibers bridging the crack,⁸ panels with 1.0% low-aspect-ratio fibers (F2V2 series) expectedly reached shear stresses lower than that of panels with 1.0% high-aspect-ratio fibers (F1V2 series), but higher than that of panels with 0.5% high-aspect-ratio fibers (F1V1 series). The trend in terms of the maximum shear stress attained for

Table 5—Summary of panel tests

ID	$f'_{c,tests}$ MPa (ksi)	v_{cr} , MPa (ksi)	γ_{cr} , $\times 10^{-3}$	v_{is} , MPa (ksi)	γ_{is} , $\times 10^{-3}$	γ_{max} , $\times 10^{-3}$	w_{ms} , mm (in.)	S_{ms} , mm (in.)	$f_{c1,max}$ MPa (ksi)	$f_{c2,max}$ MPa (ksi)	$f_{c1,fail}$ MPa (ksi)	$f_{sx,max}$ MPa (ksi)	$f_{sy,max}$ MPa (ksi)
CMS	45.2 (6.56)	2.06 (0.299)	0.183	5.99 (0.869)	8.58	8.58	0.20 (0.008)	72.1 (2.84)	1.99 (0.289)	-12.54 (-1.82)	1.04 (0.151)	270 (39.2)	622 (90.2)
CRC	45.5 (6.60)	1.37 (0.199)	0.158	5.63 (0.817)	9.77	9.87	0.39 (0.015)	70.0 (2.76)	2.04 (0.296)	-13.48 (-1.96)	-0.11 (-0.016)	330 (47.9)	633 (91.8)
F1V1MS	55.9 (8.11)	2.18 (0.316)	0.147	3.34 (0.484)	4.07	4.07	0.19 (0.007)	148.8 (5.86)	2.52 (0.365)	-7.16 (-1.04)	1.54 (0.223)	170 (24.7)	—
F1V1RC	56.1 (8.14)	1.27 (0.184)	0.160	3.13 (0.454)	4.51	4.51	0.34 (0.013)	126.0 (4.96)	2.65 (0.384)	-7.48 (-1.08)	1.03 (0.149)	195 (28.3)	—
F1V2MS	58.1 (8.43)	1.81 (0.263)	0.138	4.65 (0.674)	4.96	4.96	0.18 (0.007)	54.8 (2.16)	3.16 (0.458)	-9.55 (-1.39)	2.29 (0.332)	220 (31.9)	—
F1V2RC	58.1 (8.43)	3.10 (0.450)	0.256	4.41 (0.640)	4.60	4.60	0.21 (0.008)	81.4 (3.20)	3.18 (0.461)	-8.50 (-1.23)	1.67 (0.242)	188 (27.3)	—
F1V3MS	50.9 (7.38)	2.34 (0.339)	0.141	4.93 (0.715)	3.40	3.40	0.12 (0.005)	96.9 (3.81)	3.37 (0.489)	-7.71 (-1.12)	3.15 (0.457)	138 (20.0)	—
F1V3RC	53.1 (7.70)	2.00 (0.290)	0.190	4.72 (0.685)	3.72	4.35	0.25 (0.010)	90.0 (3.54)	3.06 (0.444)	-8.47 (-1.23)	2.59 (0.376)	178 (25.8)	—
F2V2MS	52.1 (7.56)	1.79 (0.260)	0.211	3.96 (0.574)	4.16	4.16	0.25 (0.010)	74.0 (2.91)	2.77 (0.402)	-7.14 (-1.04)	2.20 (0.319)	149 (21.6)	—
F2V2RC	52.9 (7.67)	1.82 (0.264)	0.146	3.47 (0.503)	2.75	4.53	0.33 (0.013)	115.0 (4.53)	2.41 (0.350)	-7.03 (-1.02)	1.59 (0.231)	163 (23.6)	—



(a) Monotonic backbone curve



(b) Cyclic envelope curve

Fig. 3—Comparison of shear stress-shear strain backbone response.

the cyclically loaded panels was consistent with that of the monotonically loaded panels.

All SFRC panels, except for Panel F1V3MS, sustained a maximum shear deformation of at least 44% of that of the control panels. Due to the non-ideal fiber distribution during mixing for the F1V3 series noted previously, Panel F1V3MS only sustained 40% of the maximum shear deformation withstood by that of the control panel. The control panels exhibited exceptionally high shear strains due to the transverse reinforcement’s significant post-yielding deformation capacity. Although the shear deformation capacity of all SFRC panels was similar, if one accounted for the likely reduced deformation capacity of the F1V3 series due to its non-ideal fiber distribution, then it appeared that concrete with lower fiber volume fractions or lower aspect ratio fibers had lower shear deformation capacity.

Principal tensile response—The influence of fiber type and fiber content was further clarified by examining the concrete principal tensile stress–principal tensile strain backbone response (refer to Fig. 4). The control panels’ maximum

principal tensile stress occurred during initial cracking and, therefore, no strain hardening behavior was exhibited. For all SFRC panels, strain hardening after cracking and significant post-cracking residual stresses were observed. By increasing the fiber content, higher maximum principal tensile stress was usually attained and substantial improvements in the concrete tensile behavior was noted. For the monotonically loaded panels with RC80/30BP fibers, the principal tensile stress plateau was higher than the control panel’s stress plateau by 50%, 130%, and 220% for a fiber content of 0.5%, 1.0%, and 1.5%, respectively.

Consistent with the shear response, concrete with low-aspect-ratio fibers did not perform as well. The residual tensile stress exhibited by concrete with 1.0% low-aspect-ratio fibers (F2V2 series) was between that of concrete with 0.5% and 1.0% high-aspect-ratio fibers.

Crack control characteristics—One of the key benefits of fiber addition is its ability to control crack propagation. Concrete by itself has no significant post-cracking strength and ductility. Discrete fibers bridge the crack and reduce

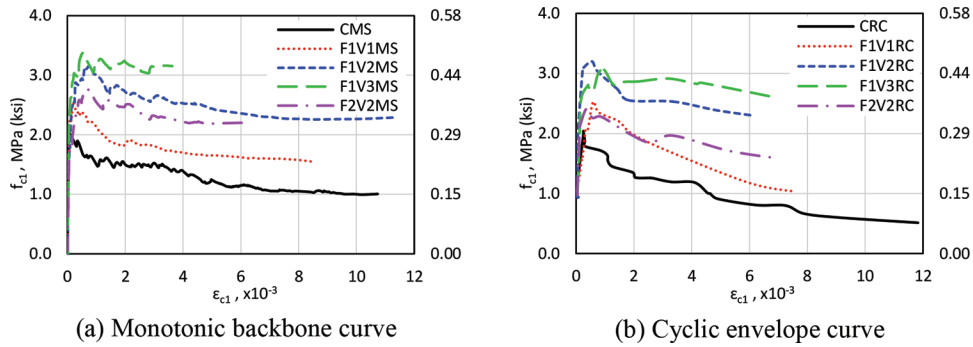


Fig. 4—Comparison of principal tensile stress-principal tensile strain backbone response.

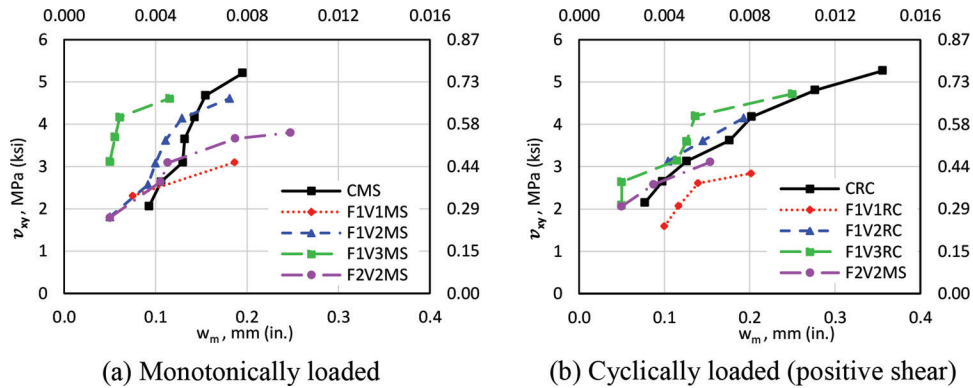


Fig. 5—Comparison of mean crack widths.

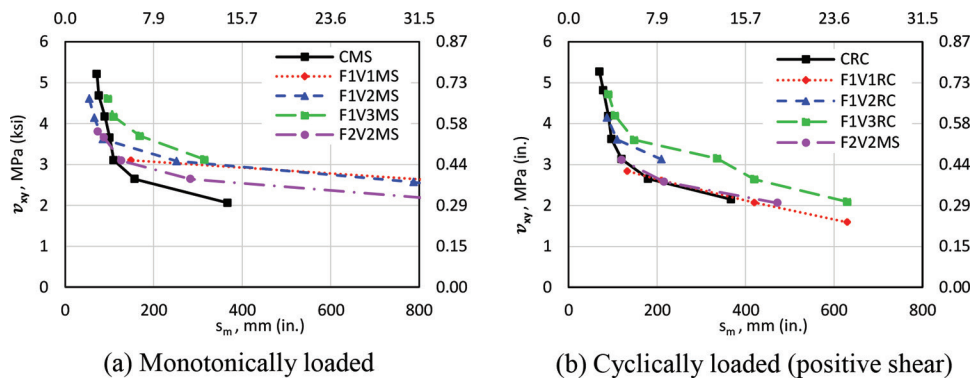


Fig. 6—Comparison of mean crack spacings.

cracking and, therefore, the post-cracking behavior of the concrete is significantly improved.

The measured average crack width and crack spacing for the panels are shown in Fig. 5 and Fig. 6, respectively. For simplicity, only the crack control parameters under positive shear are shown for the cyclically loaded panels; the cyclic crack control characteristics were similar between positive shear and negative shear.¹⁶ With higher fiber contents, smaller crack widths were developed and hence, the integrity of the cracked panel was better maintained, leading to higher shear stresses. A comparison between panels with 1.0% ZP305 fibers (F2V2 series) and panels with 1.0% RC80/30BP fibers (F1V2 series) revealed that fibers with lower aspect ratios developed noticeably larger crack widths under the same shear stress. Consistent with the stress-strain response, the crack control ability of 1.0% ZP305 fibers was between 0.5% and 1.0% RC80/30BP fibers.

Compared to the control panels, the addition of 1.0% RC80/30BP fibers allowed the concrete to exhibit comparable or slightly improved crack control capabilities under the same shear stress. With a fiber content of 1.5%, the concrete exhibited noticeably smaller crack widths compared to the control panel; this was remarkable considering the absence of transverse reinforcement in the SFRC panels.

Examination of the average crack spacing also revealed another influence of fiber addition (refer to Fig. 6). Under monotonic loading, at high shear stress levels, the SFRC panels generally exhibited smaller crack spacings than the control panels. As a result of fiber bridging, the smaller crack spacings allowed crack openings to be better controlled, enabling additional cracks to be developed and the integrity of the specimen to be maintained. Increasing the fiber content or fiber aspect ratio led to smaller crack spacings, consistent with the crack width trends. The cyclic envelope

crack spacing data shown in Fig.6(b) were more scattered and no discernible trends were observed.

Influence of loading history

Shear resistance and ductility—The complete shear stress-shear strain response for the five pairs of panels tested are shown in Fig. 7. Under increasing loads, all panels showed gradual softening with progressive stiffness degradation. The degree of pinching of the hysteretic loops was more pronounced under higher loads. Evident from the higher peak strain attained during the second cycle of the double cycle, the degree of creep was also larger under higher loads. The pinching of the hysteretic loops were similar for all SFRC panels, but were much more pronounced for the control panel.¹⁶ Hence, under small shear reversals, enhanced energy dissipation capacity without the presence of transverse reinforcement can be attained with sufficient amounts of fiber addition (1.0% to 1.5%). As discussed previously, a fiber addition of 0.5% cannot provide adequate shear resistance.

The plain concrete panel, CRC, experienced minor stress degradation; the ultimate shear stress attained was reduced by 6% compared to its monotonic counterpart. However, the ultimate shear strain increased by 14%. A strength degradation was expected due to the effects of load cycling. The primary causes of the strength degradation were the deterioration of the concrete at the crack, which led to the breakdown of the aggregate interlock mechanism, and the bond deterioration between the concrete and the steel reinforcement.

The SFRC panels exhibited minor strength degradation similar to the control panels. Overall, concrete with higher fiber contents experienced lower strength degradation. Concrete containing 0.5%, 1.0%, and 1.5% RC80/30BP fibers exhibited 6%, 5%, and 4% strength degradation, respectively. More importantly, for the panel with 0.5% fiber content, stress degradation occurred shortly after cracking and thereafter, the cyclic envelope curve constantly lagged behind the monotonic backbone curve. The panel with 1.5% fiber content, on the other hand, experienced nearly zero stress degradation until failure. The panel with low-aspect-ratio fibers, F2V2RC, experienced the largest strength degradation (12%) and the stress degradation occurred only near failure; its resistance to cyclic deteriorations did not match panels with higher-aspect-ratio fibers but was better than the panel with a lower fiber content.

No discernible trends were observed for the ultimate shear strain as a result of the cycling of load. For example, compared to its monotonic counterpart, Panel F2V2RC experienced a 34% decrease in the ultimate shear strain but the maximum shear strain increased by 9%. This indistinct trend regarding ultimate shear strain was expected, as the failure of SFRC panels was initiated by fiber pullout. Hence, the failures were largely strain-controlled and panels made of the same concrete failed under a similar level of shear deformation regardless of the loading history.

The aforementioned observation indicated the ability of SFRC members to resist cyclic loading with minor cyclic deterioration. This is contrary to the substantial cyclic deterioration observed in the single pilot test performed by Carnovale and Vecchio.¹⁴ The testing of that panel, DCP4,

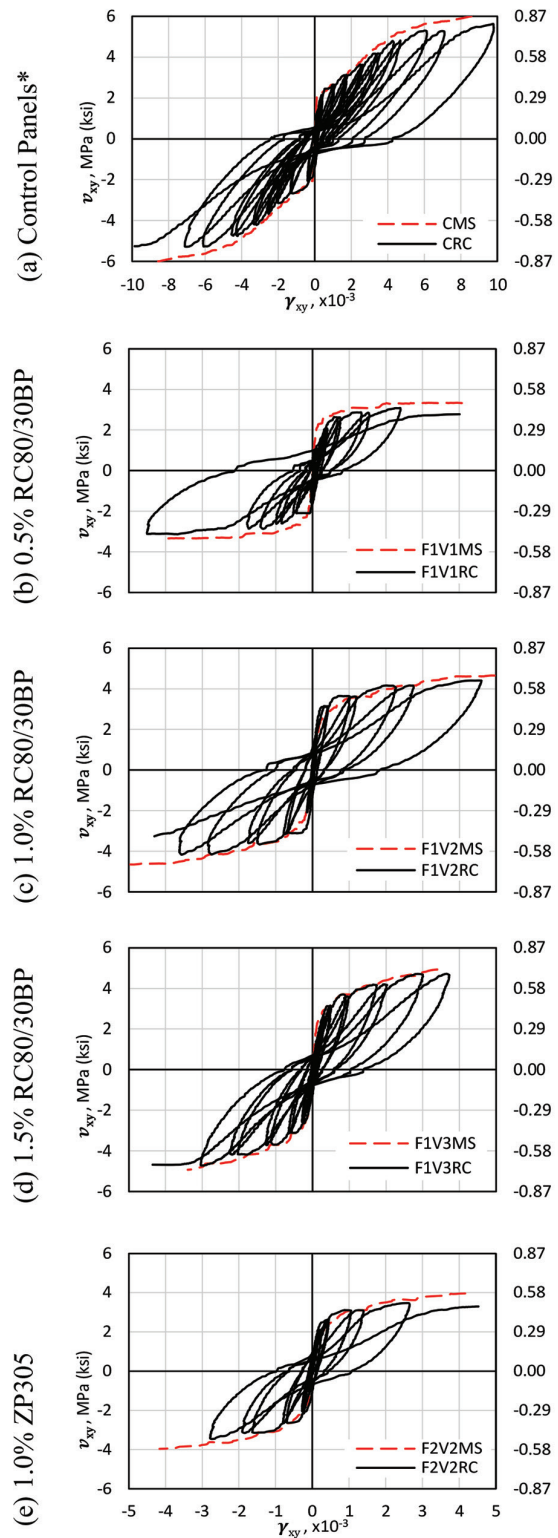


Fig. 7—Shear response of panels. (Note: Horizontal axis of (a) is different from the rest.)

was interrupted due to a hydraulic cylinder failure, which temporarily applied a non-pure-shear loading condition to the specimen. It is now believed that the response of the panel was compromised as result of this incident.

Principal tensile response—The principal tensile response for the five pairs of panels is shown in Fig. 8. All cyclically loaded panels reached a maximum principal tensile stress

similar to that of their monotonic counterpart, with cyclic degradation occurring thereafter. Consistent with the shear stress-shear strain response, the monotonic principal tensile curve was similar to the cyclic envelope principal tensile curve for each pair of panels.

No discernible trends on the influence of fiber content on the cyclic damage were observed. The panel with the lower-aspect-ratio fiber, F2V2RC, experienced the largest degradation of residual tensile load-carrying capacity. This further demonstrated that concrete with higher-aspect-ratio fibers can provide better resistance to cyclic deterioration.

Crack control characteristics—The crack widths of all cyclically loaded panels were larger than their monotonic counterpart's, demonstrating the negative effects as a result of the cycling of load (refer to Fig. 9). The larger crack widths of the cyclically loaded panel inhibited the ability of fibers to transmit stress across the cracks, which in turn reduced the specimen's ability to generate further cracking. The higher maximum shear strain of the cyclically loaded panels was in part due to their larger cyclic crack widths.

The crack width under negative shear was similar but always larger than that of positive shear. This is because the reversed cyclic loading protocol always begins in the positive shear direction, resulting in the panel being more damaged by the time it reached the same load in the negative direction.

In terms of the crack width, no discernible trend was apparent with regards to the influence of fiber type or fiber content on the degradation effects of the cycling of load. The panel with 0.5% fiber addition, F1V1RC, exhibited the largest negative shear crack widths. This occurred because under negative shear, only a few wide cracks were developed and were concentrated at the bottom half of that panel. Near failure, the panel exhibited a sudden opening of various small cracks and a more uniform crack distribution and hence, a rapid decrease in the negative average cracks widths. The above further signified the inability of SFRC with low fiber contents to produce uniform cracks, especially under reversed cyclic loadings.

SUMMARY AND CONCLUSIONS

The influence of steel fiber addition on the reversed cyclic shear behavior of SFRC was experimentally investigated through a series of 10 panel tests. The parameters of study included the fiber content, fiber aspect ratio, and loading protocol. The intent of the investigation was to improve understanding of the material under cyclic loading and to provide data useful for developing or verifying constitutive models.

Based on the findings of this experimental program, the following concluding remarks are made:

1. For end-hooked steel fibers, a high dosage (fiber content of 1.0% to 1.5%) of thin fibers (fiber aspect ratio of 79) produced the best results in terms of enhancement of shear strength and behavior. Within the samples studied, the combinations of fiber content and fiber type that gave the highest fiber count were most effective.

2. Under reversed cyclic loading, the SFRC panels exhibited stable hysteretic response with insignificant strength degradation and no noticeable changes in ductility. With the exception of panels with a fiber content of 0.5%, all panels'

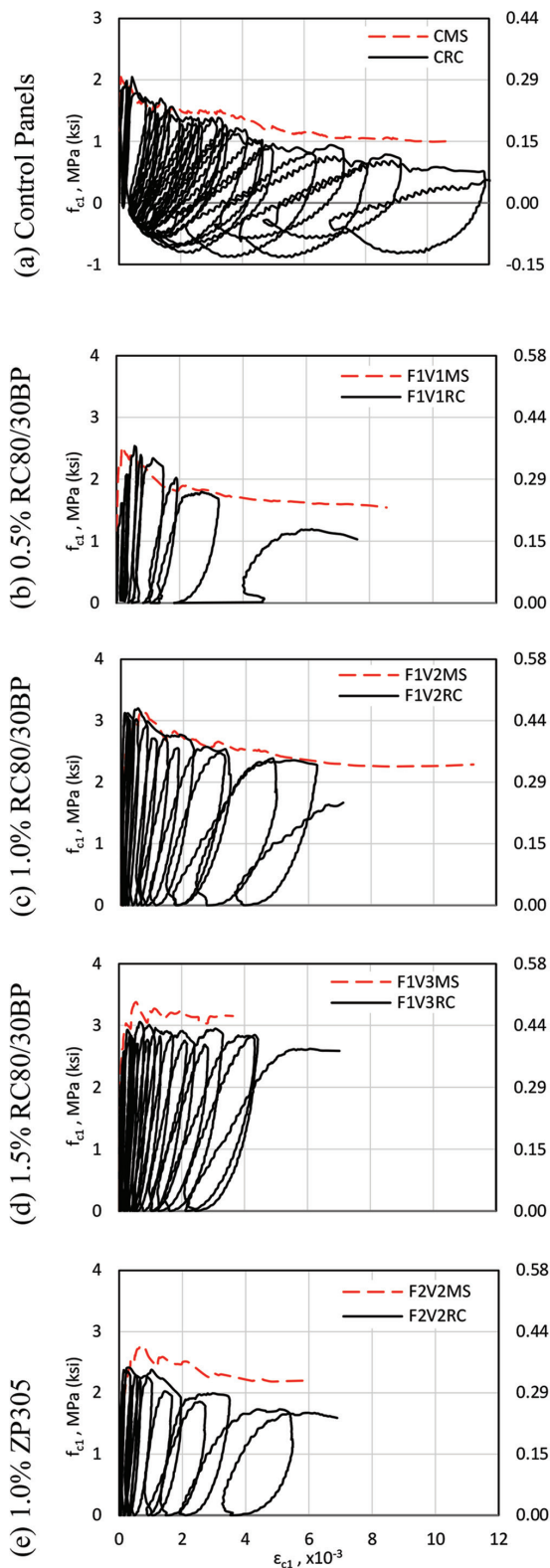


Fig. 8—Principal tensile response of panels.

monotonic backbone curve closely matched the reversed cyclic envelope curve.

3. Concrete with a fiber content of 0.5% and no transverse reinforcement did not provide adequate shear resistance, especially under reversed cyclic loading conditions; the degree of cyclic deterioration was noticeably higher for this concrete.

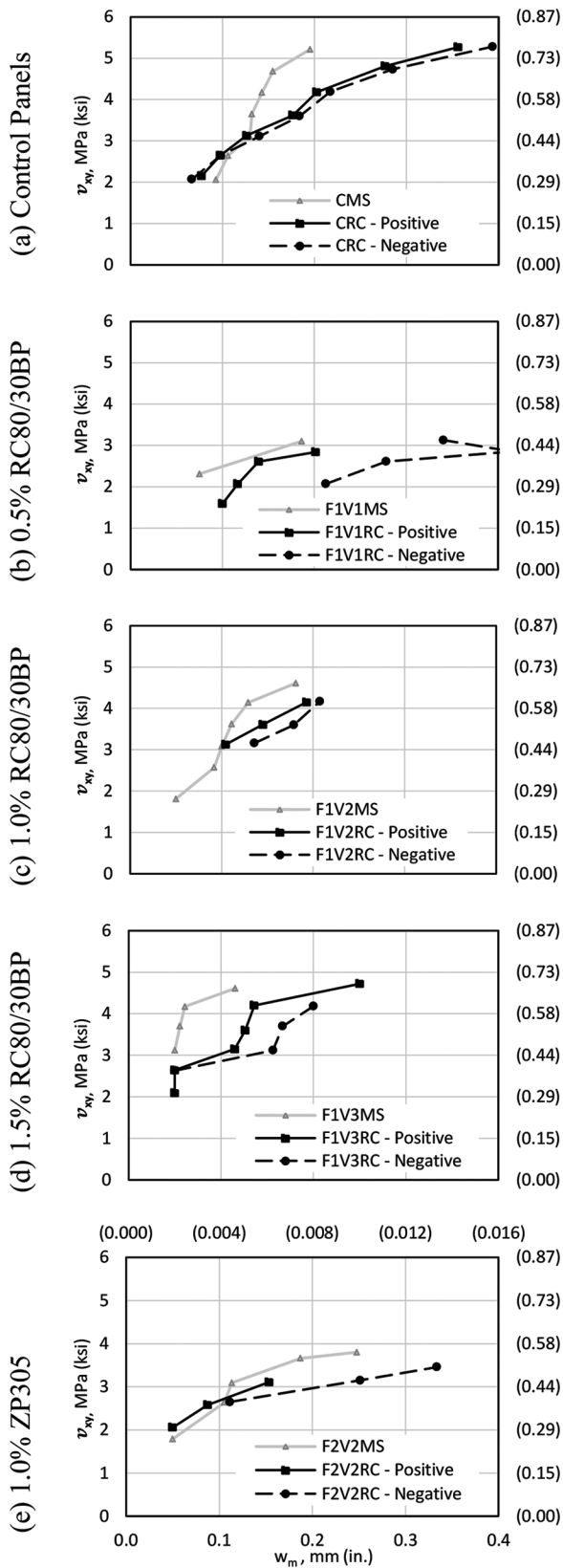


Fig. 9—Crack widths of panels.

4. SFRC panels containing a fiber content of 1.5% withstood maximum shear stresses of levels approaching those sustained by conventionally reinforced panels with a transverse reinforcement ratio of 0.42%. However, concrete with this fiber content may be more likely to experience non-ideal fiber distribution.

5. The strength capacities and tolerances for cyclic damage observed suggest that short, thin, end-hooked steel fibers with a high fiber content may be used in place of low percentages of conventional transverse steel reinforcement (for example, less than 0.4%) in the design of capacity-based members, regardless of the loading protocol.

6. SFRC panels were able to achieve approximately half or less of the maximum shear strain exhibited by the conventionally reinforced panels.

7. This lack of ductility suggested the use of steel fibers for the full replacement of low to moderate amounts of transverse reinforcement for deformation-critical members, such as the ductile element of a seismic-force-resistant system, may not be advisable until further study.

8. Ductility concerns aside, significant reductions in transverse steel requirements are feasible with the addition of steel fibers.

AUTHOR BIOS

Jun Wei Luo is a Structural Engineer-in-Training at Grubb Engineering Corporation, Red Deer, AB, Canada. He received his bachelor's and master's degrees in civil engineering from the University of Toronto, Toronto, ON, Canada. His research interests include shear behavior of reinforced concrete and analysis of fiber-reinforced concrete.

Frank J. Vecchio, FACI, is a Professor in the Department of Civil Engineering at the University of Toronto. He is a member of Joint ACI-ASCE Committees 441, Reinforced Concrete Columns, and 447, Finite Element Analysis of Reinforced Concrete Structures. He received the 1998 ACI Structural Research Award, the 1999 ACI Structural Engineer Award, and the 2011 ACI Wason Medal for Most Meritorious Paper. His research interests include advanced constitutive modeling and analysis of reinforced concrete, assessment and rehabilitation of structures, and response under extreme loads.

ACKNOWLEDGMENTS

This project was funded by the Natural Sciences and Engineering Research Council of Canada (NSERC) under the Collaborative Research and Development Grant program with Hatch Ltd. being the industrial partner. In addition to the funding provided by NSERC, the authors would like to gratefully acknowledge the material donations made by N.V. Bekaert S.A., BASF Canada, and Holcim Canada Inc.

NOTATION

A_s	=	area of reinforcing steel
AR_f	=	aspect ratio of fibers
d_b	=	diameter of reinforcing steel
d_f	=	diameter of fibers
E_s	=	modulus of elasticity of reinforcement
f'_c	=	compressive strength of concrete
$f'_{c,test}$	=	compressive strength of concrete on panel test day
f_{c1}	=	principal tensile stress of concrete
$f_{c1,fail}$	=	principal tensile stress of concrete at failure
$f_{c1,max}$	=	maximum principal tensile stress of concrete
$f_{c2,max}$	=	maximum principal compressive stress of concrete
$f_{sx,max}$	=	maximum x-direction reinforcement stress
$f_{sy,max}$	=	maximum y-direction reinforcement stress
f_u	=	ultimate tensile strength of reinforcement
f_{uf}	=	ultimate tensile strength of fibers
f_y	=	yield strength of reinforcement
l_f	=	length of fibers
s_m	=	mean crack spacing at failure
V_f	=	fiber-volume fraction
v_{cr}	=	cracking shear stress
v_u	=	ultimate shear stress
v_{xy}	=	shear stress
w_m	=	mean crack width at failure
ϵ_{c1}	=	principal tensile strain
ϵ_u	=	ultimate strain
ϵ_y	=	yield strain
γ_{cr}	=	cracking shear strain
γ_{max}	=	maximum shear strain

- γ_{ur} = shear strain correspond to ultimate shear stress
- γ_{xy} = shear strain
- ρ_x = reinforcement ratio in x-direction
- ρ_y = reinforcement ratio in y-direction

REFERENCES

1. Minelli, F., "Plain and Fiber Reinforced Concrete Beams under Shear Loading: Structural Behavior and Design Aspects," PhD dissertation, University of Brescia, Brescia, Italy, 2005, 429 pp.
2. Shah, S. P., and Rangan, B. V., "Fiber Reinforced Concrete Properties," *ACI Journal Proceedings*, V. 68, No. 2, Feb. 1971, pp. 126-137.
3. Grzybowski, M., and Shah, S. P., "Shrinkage Cracking on Fiber Reinforced Concrete," *ACI Materials Journal*, V. 87, No. 2, Mar.-Apr. 1990, pp. 138-148.
4. Susetyo, J., "Fibre Reinforcement for Shrinkage Crack Control in Prestressed, Precast Segmental Bridges," PhD dissertation, University of Toronto, Toronto, ON, Canada, 2009, 502 pp.
5. Meda, A.; Minelli, F.; Plizzari, G. A.; and Riva, P., "Shear Behaviour of Steel Fibre Reinforced Concrete Beams," *Materials and Structures*, V. 38, No. 3, 2005, pp. 343-351. doi: 10.1007/BF02479300
6. Lee, S. C.; Cho, J. Y.; and Vecchio, F. J., "Simplified Diverse Embedment Model for SFRC Elements in Tension," *ACI Materials Journal*, V. 110, No. 4, July-Aug. 2013, pp. 403-412.
7. Parra-Montesinos, G. J., "Shear Strength of Beams with Deformed Steel Fibers," *Concrete International*, V. 28, No. 11, Nov. 2006, pp. 57-66.
8. Susetyo, J.; Gauvreau, P.; and Vecchio, F. J., "Effectiveness of Steel Fiber as Minimum Shear Reinforcement," *ACI Structural Journal*, V. 108, No. 4, July-Aug. 2011, pp. 488-496.
9. ACI Committee 318, "Building Code Requirements for Structural Concrete (ACI 318-08) and Commentary," American Concrete Institute, Farmington Hills, MI, 2008, 473 pp.
10. Minelli, F., and Vecchio, F. J., "Compression Field Modeling of Fiber-Reinforced Concrete Members under Shear Loading," *ACI Structural Journal*, V. 103, No. 2, Mar.-Apr. 2006, pp. 244-252.
11. Aoude, H.; Belghiti, M.; William, D. C.; and Mitchell, D., "Response of Steel Fiber-Reinforced Concrete Beams with and without Stirrups," *ACI Structural Journal*, V. 109, No. 3, May-June 2012, pp. 359-367.
12. Chalioris, C. E., "Steel Fibrous RC Beams Subjected to Cyclic Deformations under Predominant Shear," *Engineering Structures*, V. 49, 2013, pp. 104-118. doi: 10.1016/j.engstruct.2012.10.010
13. Setkit, M., "Seismic Behavior of Slender Coupling Beams Constructed with High-Performance Fiber-Reinforced Concrete," PhD thesis, University of Michigan, Ann Arbor, MI, 2012, 261 pp.
14. Carnovale, D., and Vecchio, F. J., "Effect of Fiber Material and Loading History on Shear Behavior of Fiber-Reinforced Concrete," *ACI Structural Journal*, V. 111, No. 5, Sept.-Oct. 2014, pp. 1235-1244.
15. Vecchio, F. J., "Disturbed Stress Field Model for Reinforced Concrete: Formulation," *Journal of Structural Engineering*, ASCE, V. 126, No. 9, 2000, pp. 1070-1077. doi: 10.1061/(ASCE)0733-9445(2000)126:9(1070)
16. Luo, J. W., "Behaviour and Analysis of Steel Fibre-Reinforced Concrete under Reversed Cyclic Loading," MASC dissertation, University of Toronto, Toronto, ON, Canada, 2014, 315 pp.
17. N.V. Bekaert S.A., "Product Data Sheet for Dramix Fibers," <http://www.bekaert.com/building>.

APPENDIX

This appendix contains supplementary figures supporting the discussion contained in the journal article entitled "Behavior of Steel Fiber-Reinforced Concrete under Reversed Cyclic Shear." Figure A1 shows the jack-and-link assembly of the Panel Element Tester, and Fig. A2 shows the reinforcement layout for the panels. The failure crack patterns for the various panel tests are shown in Fig. A3.

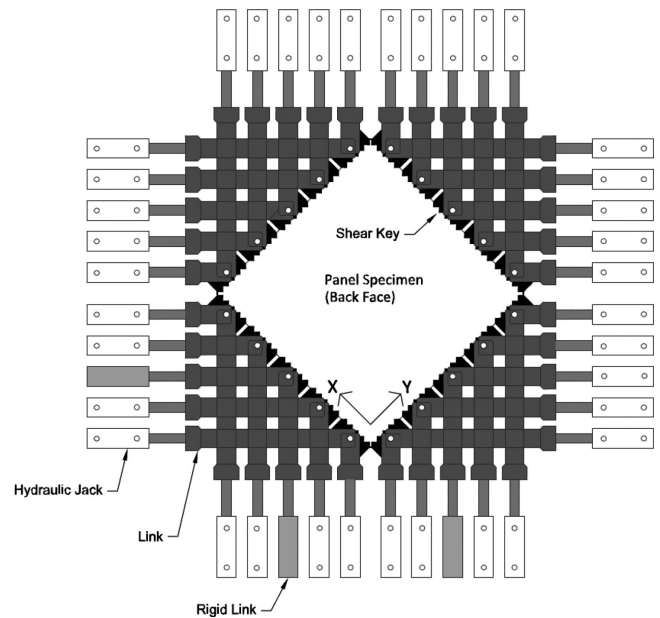
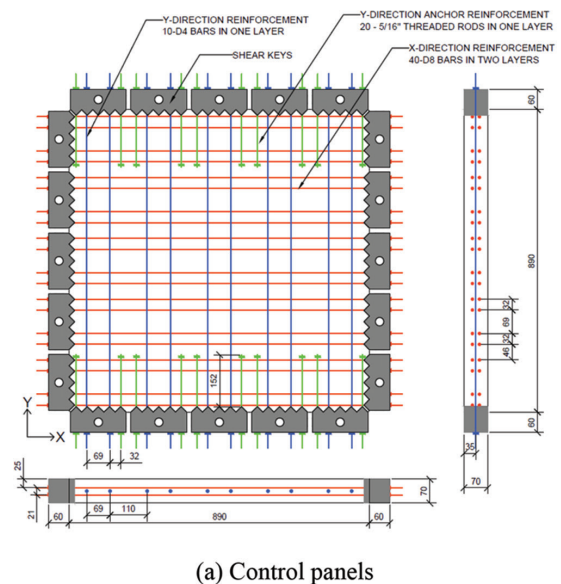
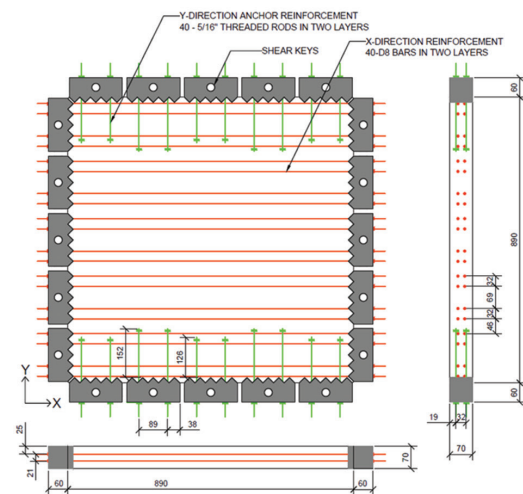


Fig. A1—Jack-and-link assembly.

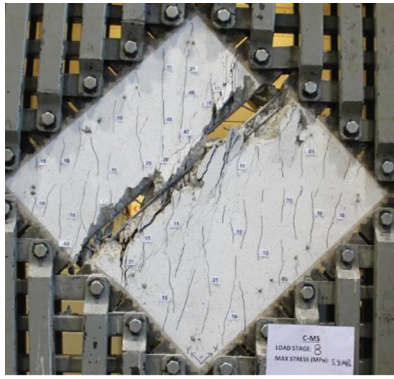


(a) Control panels

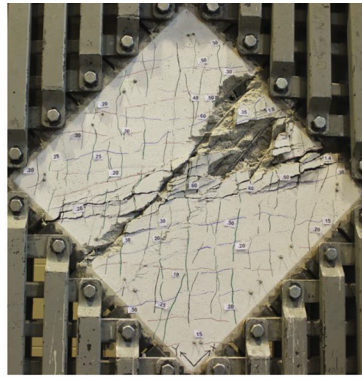


(b) SFRC panels

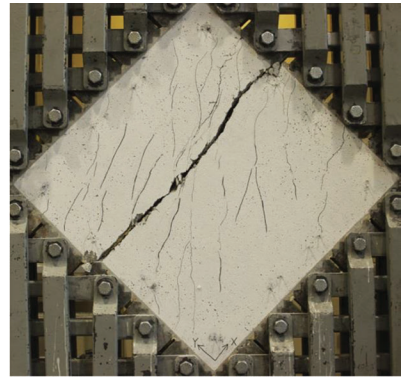
Fig. A2—Panel specimen specifications. (Note: All dimensions in mm; 1 mm = 0.0394 in.)



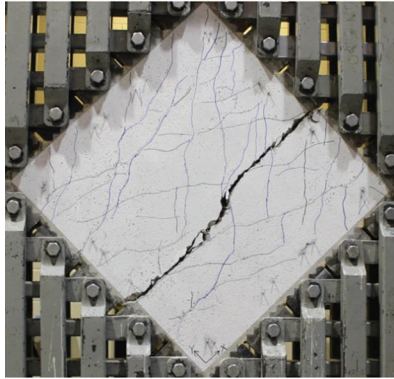
(a) CMS



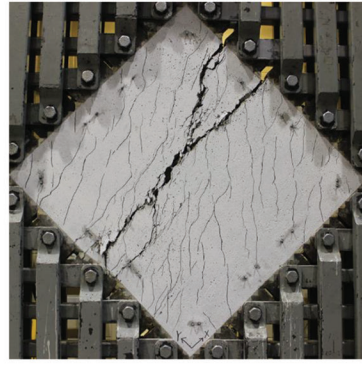
(b) CRC



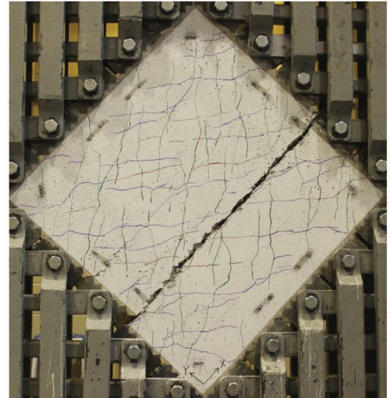
(c) F1V1MS



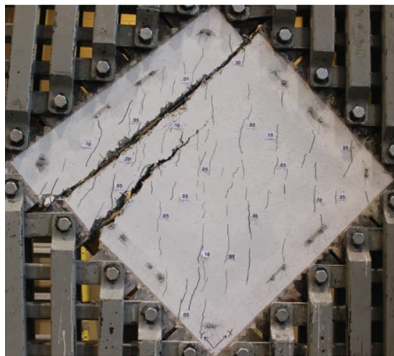
(d) F1V1RC



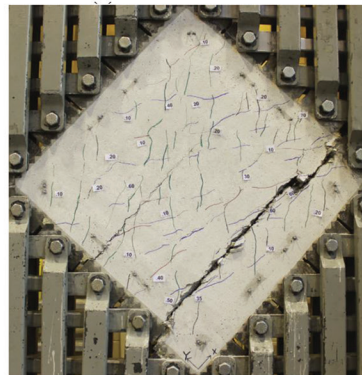
(e) F1V2MS



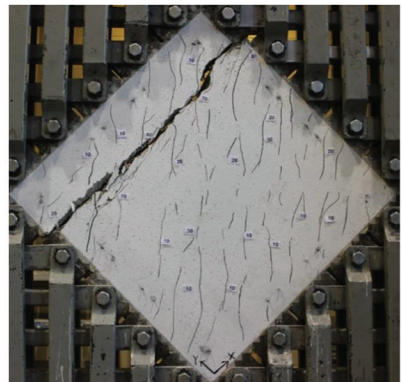
(f) F1V2RC



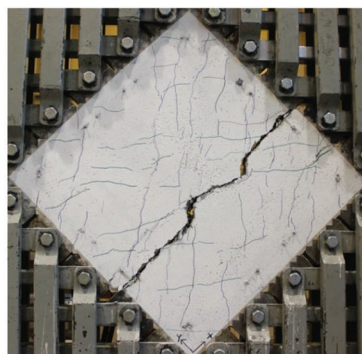
(g) F1V3MS



(h) F1V3RC



(i) F2V2MS



(j) F2V2RC

Fig. A3—Panel failure crack patterns.

Reproduced with permission of the copyright owner. Further reproduction prohibited without permission.